- 1 Cell surface-expression of the phosphate-binding protein PstS: System
- 2 development, characterization, and evaluation for phosphorus removal and
- 3 recovery

5 Faten B. Hussein<sup>1</sup>, Kaushik Venkiteshwaran<sup>1</sup>, Brooke K. Mayer<sup>1,\*</sup>

6

Department of Civil, Construction and Environmental Engineering, Marquette University
 1637 W Wisconsin Ave, Milwaukee, WI 53233

9

\* Correspondence should be addressed to Brooke K. Mayer: <u>brooke.mayer@marquette.edu</u>

**Abstract:** Simultaneous overabundance and scarcity of inorganic phosphate (P<sub>i</sub>) is a critical issue driving the development of innovative water/wastewater treatment technologies that not only facilitate P<sub>i</sub> removal to prevent eutrophication, but also recover P<sub>i</sub> for agricultural reuse. Here, a cell-surface expressed high-affinity phosphate binding protein (PstS) system was developed, and its P<sub>i</sub> capture and release potential was evaluated. E. coli was genetically modified to express PstS on its outer membrane using the ice nucleation protein (INP) as an anchoring motif. Verification of protein expression and localization were performed utilizing SDS-polyacrylamide gel electrophoresis (SDS-PAGE), western blot, and outer membrane separation analyses. Cell surface characterization was investigated through acid-base titration, X-ray photoelectron spectroscopy (XPS), and Fourier transform infrared spectroscopy (FTIR). These tests provided information on the macromolecular structure and composition of the bacteria surface as well as the protonexchange properties of the surface functional groups (i.e., pKa values). Phosphate desorption and adsorption batch experiments were conducted to evaluate the effects of temperature, pH, and ionic strength on phosphate capture and release. The PstS surface-displayed cells demonstrated greater potential to release and capture phosphate compared to non-modified cells. Higher temperatures up to 40°C, basic pH conditions (pH = 10.5), and higher ionic strength up to 1.0 mol/L KCl promoted 20% to 50% higher phosphate release.

28 29

12

13

14

15

16

17

18

19

20

21

22

23

24

25

26

27

#### 30 **Keywords:**

- 31 Phosphorus recovery
- Water treatment
- 33 Eutrophication
- 34 Surface-expression
- 35 PstS protein
- 36 E. coli bacteria
- 37 Phosphate

# Introduction

Inorganic phosphate ( $P_i$ ) is an essential nutrient for all living organisms. However, its simultaneous overabundance and scarcity leads to a "phosphorus paradox," wherein excess concentrations of  $P_i$  in water bodies cause eutrophication, while available supplies of nonrenewable phosphate rock for agricultural use are continuously depleted. Surplus  $P_i$  ultimately leads to eutrophication and the subsequent development of hypoxia (Cai et al., 2011; Mayer et al., 2013; Rittmann et al., 2011). Eutrophication affects water quality and alters ecosystem structures in freshwaters worldwide (Dodds et al., 2009). A number of technologies have been developed to remove  $P_i$  from water, e.g., selective and non-selective adsorptive materials, ion exchange resins, and biological materials (i.e., whole-cell microbes or proteins) (Mayer et al., 2013). These technologies focus on *removing* pollutant  $P_i$  from nonpoint sources (e.g., runoff from urban and agricultural lands) and point sources (e.g., municipal and industrial wastewater treatment facilities) to meet phosphorus regulations and guidelines in natural waters and treated discharges, respectively. The ability of these strategies to *recover and reuse* the  $P_i$  removed from water is also critical in reducing demands for nonrenewable phosphate rock (Mayer et al., 2016).

One interesting approach to P<sub>i</sub> removal and recovery from water is the development of systems harnessing the use of the high-affinity phosphate binding protein PstS (also known by the acronym PBP) (Choi et al., 2013; Kuroda et al., 2000; Li et al., 2009; Venkiteshwaran et al., 2018; Yang et al., 2016). Bacterial PstS is one of four proteins that comprise the Pst complex (Luecke and Quiocho, 1990). The periplasmic PstS protein binds phosphate in a deep cleft using 12 hydrogen bonds, which provides strong, highly-selective binding affinity (which is extraordinarily selective even in the presence of other wastewater oxyanions such as sulfate and arsenate) (Ledvina et al., 1998; Luecke and Quiocho, 1990). Several PstS protein systems have been tested to evaluate P<sub>i</sub> removal efficiency from water. Kuroda et al. (2000) immobilized PstS on sepharose beads, and found removal of <sup>32</sup>P-labeled phosphate to below the detection limit (9.5 ng-P/L) using packed columns filled with the modified beads. Choi et al. (2013) evaluated *in vivo* PstS, using recombinant *E. coli* to overexpress PstS in the cell's periplasmic space. The recombinant *E. coli* efficiently removed P<sub>i</sub> (>94% removal), even when starting at low phosphate concentrations, ranging from 0.2 to 1.0 mg/L. In a third variation, recombinant *E. coli* was modified to express PstS on the cell surface (as opposed to the natural location in the periplasmic space) using the ice

nucleation protein (INP) as an anchoring protein (Li et al., 2009). This cell surface-expressed system provided 5% phosphate removal using an influent concentration of 500 mg-PO<sub>4</sub><sup>3-</sup>/L (Li et al., 2009).

Beyond removal alone, our research group recently conducted P<sub>i</sub> recovery studies using PstS proteins immobilized on beads (Venkiteshwaran et al., 2018) and recombinant *E. coli* overexpressing PstS protein in the periplasmic space (Yang et al., 2016). The extracellular PstS system using proteins immobilized on the bead surface was more conducive to P<sub>i</sub> recovery compared to the periplasmic PstS system. Thus, we hypothesized that exposing the PstS directly to the water matrix by expressing the protein on the cell surface would facilitate P<sub>i</sub> release in comparison to periplasmic PstS (in which case the cell membrane and perhaps cytoplasmic regulation could impede PstS release). No studies have yet investigated conditions targeting P<sub>i</sub> removal and recovery using cell surface-displayed PstS proteins. Accordingly, the objectives of this study were: 1) to establish and characterize the cell surface-expressed PstS system, and 2) to evaluate P<sub>i</sub> removal and release under controlled experimental conditions varying temperature, pH, and ionic strength using cell surface-expressed PstS.

# 1. Materials and Methods

#### 1.1 Bacterial Strains, Plasmids, and Culture Conditions

*E. coli* strain DH5α was used as the host for the recombinant plasmid, while strain BL21 (AI) was used for protein expression. The gene sequences of INP (N terminus) and PstS were synthesized and subcloned into plasmid pTrcHis\_B (as confirmed by Thermofisher, USA). INP was selected as the anchoring motif as it is characterized by stable expression and modifiable internal repeating units (Jung et al., 1998). Plasmid pTrcHis\_B was used for the construction and expression of the fusion protein (INP + PstS). A hexa histidine tag (6xHis-tag) was inserted before the fusion protein gene sequence to facilitate western blot analysis using a specific anti-His antibody (the gene map is shown in Supplementary Data **Fig. S1**). The recombinant plasmid was transformed into DH5α and BL21 (AI) using a heat-shock procedure (Invitrogen Life Technologies manual C6070-03). Briefly, 2 μL of the recombinant plasmid was added to 50 μL of cells and gently mixed. The reaction tube was kept in ice for 30 min and then immersed in a water bath at 42°C for 45 sec. The reaction tube was then returned to ice for 2 min. Afterward, 250 μL of Luria-Bertani (LB) medium

was added to the reaction tube and incubated at 37°C for 1 hr. The incubated cells were spread on LB agar containing ampicillin and left overnight at 37°C. Isolated colonies were collected, introduced into 10 mL LB, and incubated overnight at 37°C. Aliquots of the culture were mixed with 70% glycerol (1:0.56 v/v, culture/glycerol) and stored at -80°C until use.

104105

106

107

108

109

110

100

101

102

103

Recombinant cells were cultivated in LB medium amended with 100  $\mu$ g/mL ampicillin at 37°C and vigorously agitated at 250 r/min. For protein induction, 1 mmol/L isopropyl  $\beta$ -D-1-thiogalactopyranoside (IPTG) was added to the cell culture once the OD<sub>600</sub> reached 0.6-0.8. The IPTG was allowed to react with the culture for 3-4 hr, after which the induced cells were centrifuged and stored at -20°C until use. An uninduced sample of the cells was tested in parallel as a control. *E. coli* BL21 (AI) cells bearing an empty pTrcHis\_B vector (no PstS or INP inserted) were used as negative control cells.

111112

113

114

115

116

117

118

119

120

121122

123

124

125

126

127

128

129

130

# 1.2 SDS-PAGE and Western Blot Analyses

SDS-polyacrylamide gel electrophoresis and western blot analyses were used to confirm the expression of PstS protein and the specificity for His-tag fusion in the induced cells. One mL of cells cultured to log phase in LB was centrifuged to prepare three different samples with final  $OD_{600} = 1$  (i.e., control cells [empty vector, expected to have natural levels of periplasmic PstS], uninduced cells [no IPTG induction, expected to express low levels of surface-expressed PstS], and induced cells [expected to overexpress PstS on the cell surface]). The resulting cell pellets were resuspended in a loading buffer (100 mmol/L Tris-HCl, pH 6.8, containing 4% SDS, 0.2% bromophenol blue, 20% glycerol, and 200 mmol/L beta-mercaptoethanol [BME]) and heated for 15 min at 98°C. The samples were loaded onto 10% SDS-PAGE gel and analyzed under 120 V for 1.5 hr. The gel cast was stained by Coomassie brilliant blue for 30 min and de-stained in 40% methanol and 10% glacial acetic acid solution to obtain a clear gel image. For western blot, proteins on the SDS-PAGE gel were transferred to a nitrocellulose membrane under 250 mA for 1.5 hr. The membrane was blocked with 1x TBS (Tris-buffered saline) containing 5% w/v nonfat dry milk and 0.1% Tween-20 at room temperature for 1 hr. The membrane was then incubated with primary rabbit anti-His antibody (Bethyl Laboratories, Inc.) overnight at 4°C. Incubation with secondary anti-rabbit immunoglobulin G (IgG) antibody (Sigma Aldrich, US) was conducted at room temperature for 1 hr. Luminol solution was added to develop the protein signal on the films.

# **1.3 Outer Membrane Separation**

To isolate the outer membrane (OM) fraction and confirm the location of the fusion protein, we followed the procedure published by Park et al. (2015). Briefly, the centrifuged *E. coli* cells were resuspended in lysozyme buffer containing 0.2 mol/L Tris-HCl (pH 8.0), 200 μg/mL lysozyme, 20 mmol/L sucrose, and 0.2 mmol/L ethylenediaminetetraacetic acid (EDTA) for 10 min at room temperature. Next, 20 μg/mL aprotinin and 1 mmol/L phenylmethylsulfonyl fluoride (PMSF) were added to the solution. An equivalent volume of extraction buffer (2% Triton X-100, 50 mmol/L Tris-HCl, 10 mmol/L MgCl<sub>2</sub>, and 10 μg/mL DNase) was added to isolate the outer membrane. After incubation in ice for 30 min, the lysate was centrifuged at 5000 r/min for 5 min; the supernatant was recentrifuged at 18,000 r/min for 10 min. The presence of PstS was assessed in the collected fractions by SDS-PAGE.

#### 1.4 Cell Surface Characterization

Cell surface characterization through acid-base titration, XPS, and FTIR were performed to provide information on the surface properties of *E. coli* cells. Acid-base titration provides proton-exchange properties of the surface functional groups (i.e., pK<sub>a</sub> values). Proton and hydroxide concentrations are more precisely obtained by acid-base titration at low detection limit compared to spectroscopic techniques (Ojeda et al., 2008). FTIR spectroscopy and XPS characterize the macromolecular structure and composition of the bacterial surface. FTIR identified potential functional groups from lipids, proteins, and carbohydrates on the cell surface. XPS was used to estimate the relative elemental surface composition. The combination of analyses offers a comprehensive understanding of the cell surface properties as an initial step toward understanding the cells' response under different conditions.

#### 1.4.1 Acid-Base Titration

Cultures of control, uninduced, and induced cells were centrifuged at 6000 r/min at room temperature and the collected pellets were washed with 0.01 mol/L NaCl. This process was repeated three times to remove LB media residue. The pellets were resuspended in a background electrolyte of 0.01 mol/L NaCl with  $OD_{600} = 2$  (~ 0.78 g bacteria/L). Samples were purged with  $N_2$  gas for 5 min to remove atmospheric  $CO_2$  gas. Next, 20 mL of bacterial suspension was

transferred to a polypropylene titration vessel. Titration was performed using an EasyPlus<sup>TM</sup> titrator (Mettler Toledo, Easy pH) at room temperature. All samples were initially acidified to pH ≈ 3.5 using 0.01 mol/L HCl, followed by titration with 0.01 mol/L NaOH to ultimately reach pH 10.5.

ProtoFit GUI 2.1 rev1 software using surface complexation models such as the constant capacitance model (CCM) and non-electrostatic model (NEM) was used to determine pK<sub>a</sub> values. The CCM requires one fit parameter (i.e., capacitance of electrical double layer) while the NEM does not require any parameters (Turner and Fein, 2006). The extended Debye-Huckel activity coefficient model was used as it is considered the most accurate model for ionic strength up to 0.1 mol/L (Langmuir, 1997). Three-site functional group and four-site functional group specifications were applied and compared for best fit simulation. The surface area of *E. coli* was calculated using an average cell length of 2  $\mu$ m and 1  $\mu$ m diameter. The cell number from the optical density reading and the dry weight of the cells were used to calculate the specific surface area (16.2 m²/g dry weight).

# 1.4.2 Macromolecular structure and composition of the bacterial surface

For X-ray photoelectron spectroscopy (XPS) analysis, E. coli cells were suspended in 10 mmol/L Tris-HCl and 1 mmol/L MgCl<sub>2</sub> at pH 7, frozen at -20°C, and freeze-dried, as previously reported (Van Der Mei et al., 2000). Frozen samples of control cells, uninduced cells, and induced cells were mounted on the bench-top freeze dryer manifold (Millrock Technology BT85A) at 150 mT and -48°C for 48 hr. The resulting powder was analyzed using a Perkin-Elmer PHI 5400 ESCA system equipped with a Mg Ka X-ray source (1253.6 eV). A wide survey scan with pass energy 100 eV and 1 eV step size was conducted for each sample, providing a path depth 2-5 nm into the surface layer. CasaXPS 2.3.19 software was used to generate the XPS spectra for all samples and calculate the surface atomic concentrations of C, N, O, and P.

For Fourier transform infrared spectroscopy (FTIR) analysis, bacterial suspensions (in 10 mmol/L Tris-HCl and 1 mmol/L MgCl<sub>2</sub> at pH 7) were examined using an IR Tracer-100 FTIR spectrometer (Shimadzu Scientific Instruments) with a KBr beam splitter. Spectra for all samples were obtained over 50 scans with a resolution of 2 cm<sup>-1</sup> and a wavenumber range from 4000 to 400 cm<sup>-1</sup>. The

193 spectrum of the background solution was subtracted from the bacterial suspensions' spectra.

Functional group presence was ascertained using corresponding peak wavenumbers.

195

196

197

198

199

200

201

202

203

204

205

206

194

# 1.5 Phosphorus Desorption and Adsorption Batch Experiments

To run the batch experiments, desorption tests were initially performed to remove legacy P<sub>i</sub> since the cells were cultured in highly concentrated P<sub>i</sub> medium (150-170 mg-PO<sub>4</sub><sup>3-</sup>/L). The cell pellets were washed with buffer (10 mmol/L Tris-HCl and 1 mmol/L MgCl<sub>2</sub> at pH 7) and centrifuged twice at 6000 r/min. The pellets were then resuspended in the same buffer at  $OD_{600} = 2$ . The desorption capacity of the control, uninduced, and induced cells was investigated at different buffer pH (3.5, 5.5, 7, 8.5, and 10.5). The effects of temperature (20, 30, and 40°C) and ionic strength (0.1, 0.3, 0.5, 0.7, 1 mol/L KCl) were also studied. In all tests, cell concentrations were maintained at  $OD_{600} = 1$ . All tests were conducted in triplicate at room temperature for 3 hr and 250 r/min mixing in Tris-HCl buffer unless otherwise specified. The final phosphate concentration in all tests was measured using the standard ascorbic acid method (APHA, 2005).

207

208

209

210

211

212

213

214

215

216

For adsorption tests, three different treatment conditions were initially applied to initiate phosphate desorption from the cells before conducting the adsorption experiments: cell starvation under low-P<sub>i</sub> conditions, variable pH and temperature, and enzymatic treatments. One set of cells was suspended in Tris-HCl buffer at pH 7 for 15 hr (starvation treatment). A second set of cells was suspended in Tris-HCl solution at pH 10 and 40°C for 3 hr (pH and temperature treatment). The last set of cells was suspended in Tris-HCl at pH 7 with 1 unit/mL polynucleotide phosphorylase (PNP) and 1 mmol/L of 7-methylguanosine for 3 hr (enzymatic treatment). All treated cells were centrifuged at 6000 r/min and resuspended in phosphate solution (either 7 mg PO<sub>4</sub><sup>3</sup>-/L or 70 mg  $PO_4^{3-}/L$ ) for 3 hr.

217

218

219

220

221

#### 1.6 Statistical Analysis

Two-way ANOVA followed by Tukey post-hoc analysis was performed to assess the differences in phosphate capture and release due to test factors, i.e., temperature, pH, ionic strength, and cell type. Nonparametric Kolmogorov–Smirnov analysis was used to compare the acid-base titration 222 curves. All statistics were performed using GraphPad Prism with a significance level of  $\alpha = 0.05$ .

# 2. Results and Discussion

#### 2.1 Confirmation of Surface Expression using SDS-PAGE, Western Blot Analyses,

# and Outer Membrane Separation

Expression of the fusion protein (INP + PstS) in the recombinant *E. coli* BL21 (AI) cells was confirmed via SDS-PAGE analysis (**Fig. 1a**). Relative to the other samples, a distinct band is visible for the induced PstS cells at a molecular weight (MW) of 60 kDa, which is the expected size of the PstS and INP proteins together. Two other notable bands are present at a MW of 35 kDa for PstS and 25 kDa for INP. Separation of the two proteins might result from protease attack on the N-terminal of the INP protein, as observed by Li et al., (2003) and Li, et al. (2009).

The specificity of the His-tag fusion was confirmed via western blotting. As shown in **Fig. 1b**, no bands were observed in the expected size ranges for either the control cells or the uninduced cells. The induced cell sample was characterized by two distinct bands at 60 kDa (full size of INP + PstS) and 25 kDa (size of INP only). These results confirmed expectations since the His-tag region of the constructed plasmid was located ahead of the InaK-N gene sequence (associated with the INP protein). Quantification of the western blot results was performed using Image Studio Lite software (version 5.2.5), and indicated that approximately 27% of the overexpressed protein was

present in the full fusion form (Supplementary Data Table S1).

To verify the location of the PstS protein, an outer membrane fractionation procedure was performed to isolate cellular fractions (Park et al., 2015). The outer membrane fraction was obtained by enzymatic treatment with lysozyme to hydrolyze the peptidoglycan layer followed by liposome isolation using Triton X-100 as a detergent. **Fig. 1c** shows the SDS-PAGE results from the outer membrane fraction and the cell lysate (from the internal cellular constituents) fractions. A distinct band is visible at 35 kDa for the outer membrane fraction, corresponding to the size of the PstS protein. Alternately, low levels of PstS protein are indicated by weak bands for the duplicate cell lysate samples. Altogether, the SDS-PAGE, western blot, and outer membrane separation analyses demonstrated successful PstS protein expression and localization on the outermost surface of the *E. coli* cells.

#### 2.2 Cell Surface Characterization

#### 2.2.1 Acid-Base Titration

The typical titration curve for all cells -- control cells (CC), uninduced cells (UC), and induced cells (IC) -- is illustrated in Fig. 2a. The curves for all cell types shifted toward the right starting at pH  $\approx$  5.5 compared to the titration curve for the background solution (electrolyte solution 0.1 M NaCl). Thus, the presence of the bacteria provided additional buffering capacity. The active functional groups on the cell surfaces provide buffering capacity as they consume additional base via deprotonation (Ngwenya et al., 2003). The titration data for the control cells was significantly different than uninduced and induced cells. The titration curve for the control cells suggests a higher presence of protonated functional groups (greater buffering capacity) on the surface compared to either the induced or uninduced cells. Fig. 2a also shows four regions characterized by different behavior, possibly indicative of different surface pK<sub>a</sub> values (i.e., below pH  $\approx$  5, between pH  $\approx$  6.2, between pH  $\approx$  6.2 and pH  $\approx$  9.4, and above pH  $\approx$  9.4).

Figs. 2b, 2c, and 2d show the three-site constant capacitance model (CCM) and three-site nonelectrostatic model (NEM) fits for the raw titration data for the control cells, uninduced cells, and induced cells, respectively. The control and uninduced cells were best fit using the CCM, whereas the induced cells were best fit using the NEM. The CCM assumes that surface charge is homogeneously distributed over the bacterial surface, giving rise to relatively simple electrostatic field behavior (Ojeda et al., 2008). Therefore, the existence of extra charged molecules on the surface (i.e., protein) might disturb the homogeneity of the surface charge distribution. The calculated pKa values from both models are listed in Table 1. Regardless of cell type, the two models predicted similar values for pK<sub>a2</sub>. However, the predicted pK<sub>a1</sub> values using the CCM were consistently lower than the values from the NEM, whereas the opposite was true for the predicted pK<sub>a3</sub> values (where CCM results were consistently higher than NEM). Sites with pK<sub>a</sub> values of 3.15 to 4.5 may be indicative of the presence of carboxyl groups, sites with pK<sub>a</sub> 5.36-6.15 would be assigned to the phosphate group, and sites with pK<sub>a</sub> 7.46-9.75 could be tentatively assigned to hydroxyl and amine groups. Reported pK<sub>a</sub> values vary for the carboxyl group from 2-6, for the phosphate group from 5.6-7.2, for the amine group 8.6-9, and for hydroxyl from 8-12 (Dittrich and Sibler, 2005; Guiné et al., 2006; Haas, 2004; Hong and Brown, 2006; Ojeda et al., 2008).

Considerable difference was observed between the pK<sub>a3</sub> values for the induced cells compared to other cells. The higher value may correlate to the presence of PstS protein on the surface of *E. coli*, which may provide an additional deprotonated functional group based on the theoretical isoelectric point (pH<sub>pzc</sub>) of PstS of 8.39 (calculated based on the sequence of amino acids, https://web.expasy.org/compute\_pi/). Alternately, the average pH<sub>pzc</sub> for unmodified *E. coli* cells is 6.6 (strain K12, from the proteome isoelectric point database [Kozlowski, 2016]). This is further demonstrated through the calculated pH<sub>pzc</sub> for the cells (**Table 1**), which demonstrated that the induced cells have a higher pH<sub>pzc</sub> value compared to the uninduced and control cells.

# 2.2.2 Macromolecular structure and composition of the bacterial surface

The XPS wide scan for the control cells, uninduced cells, and induced cells is shown in Fig. 3a. The overlying spectra reveal many peaks identified as C, N, and O elements, with other peaks identified as Cl, S, and P. Notably, the outermost cell surface (2-5 nm penetration depth) contains mainly C, N, and O. The carbon peak can indicate a carboxylic group R-COO-, and the oxygen peak may be attributed to a single-bond oxygen in hydroxide or an acetal group (Ojeda et al., 2008). The nitrogen peak likely represents amine or amide groups characteristic of proteins, and the phosphorus can be attributed to phosphate groups (Dufrêne et al., 1997; Omoike and Chorover, 2004; Van Der Mei et al., 2000). The atomic composition of the bacterial surface resulting from the integration of the  $C_{1s}$ ,  $N_{1s}$ ,  $O_{1s}$ , and  $P_{1s}$  peaks is listed in Fig. 3a. The values of total carbon were similar for induced and uninduced cells, at approximately 10% more than the control cells. Other compositions varied amongst the cell types. The oxygen content was higher in control cells compared to induced and uninduced cells, whereas the nitrogen content was lower in control cells compared to the other cells. This ostensibly stems from the addition of the fusion protein (the backbone structure of which is a combination of amino acids, i.e., carbon and nitrogen constituents) in the induced and uninduced cells. Although XPS analysis provided quantitative characterization of the surface composition, the results are highly sensitive and can vary due to minor variations such as  $OD_{600}$  readings, peak limits, and the cell pellet washing procedure.

The FTIR spectrum conveys molecular-level information about the functional groups on the cell surface (**Fig. 3b**; peak functional group assignments are listed in the Supplementary Data **Table S2**). As all cells were from the same strain, similar FTIR spectra were expected, with slight

differences between the cell types as a result of protein overexpression. The spectrum for the induced cells exhibited higher intensity peaks in the protein region (~1400-1700 cm<sup>-1</sup>). Three functional groups were identified in this region: C=O stretching in amides (amide I at wavenumber ≈1654 cm<sup>-1</sup>), N-H bending and C-N stretching in amides (amide II at wavenumber ≈1540 cm<sup>-1</sup>), and C-H deformation of methylene (CH<sub>2</sub>) or methyl (CH<sub>3</sub>) groups of proteins at wavenumber ≈1455 cm<sup>-1</sup>. Additionally, a hydroxyl group peak was identified (COOH at wavenumber ≈1270 cm<sup>-1</sup>). The outcomes of FTIR spectra were consistent with previous examinations of cell surfaces of different bacterial strains (Dittrich and Sibler, 2005; Filip et al., 2008; Jiang et al., 2004).

Results from the cell surface characterization analyses can inform more mechanistic linkages between the surface-expressed system and its associated phosphate removal and recovery capabilities.

# 2.3 Phosphorus Desorption Batch Experiments

Before initiating adsorption tests, P<sub>i</sub> desorption was performed to prepare the proteins for effective P<sub>i</sub> capture, analogous to the regeneration phase of phosphate ion exchange media. Thus, desorption tests were initially conducted to remove legacy P<sub>i</sub> since the cells were cultured in highly concentrated P<sub>i</sub> medium (150-170 mg-PO<sub>4</sub><sup>3-</sup>/L). As detailed in the following sections, the use of an active cell-based system introduced potential for variations in the influence of temperature, pH, and ionic strength not only on phosphate capture and release using the surface-expressed PstS proteins, but also on the cell's basic functions related to P<sub>i</sub> uptake and release. For simplicity, we have adopted the terms "adsorption" and "desorption" to characterize P<sub>i</sub> capture and release, while recognizing that multiple mechanisms are actually at play in this cellular system.

#### 2.3.1 Effect of Temperature

Phosphorus desorption from control cells, uninduced cells, and induced cells as a function of temperature is illustrated in **Fig. 4a**. Increasing the temperature to 40°C promoted release of P<sub>i</sub> from all cells, yielding approximately 5-6 times greater release than at 20°C. Yang et al. (2016) also reported an increase in P<sub>i</sub> release by *E. coli* cells as a function of temperature. At 40°C, the induced cells desorbed approximately 20% more P<sub>i</sub> compared to the control cells. There was a significant difference between P<sub>i</sub> release among the three cell types as a function of temperature, with higher

temperatures promoting desorption (p = 0.001). However, there was no significant difference between  $P_i$  desorbed from the uninduced cells and control cells at  $20^{\circ}$ C (p = 0.64) and  $30^{\circ}$ C (p = 0.29).

350351

352

353

354

355

356

357

358

359

360

347

348

349

Increasing temperature increases the rate of cellular biochemical activity, and this activity depends on ATP hydrolysis/synthesis. The product of ATP hydrolysis is a free  $P_i$  ion that can be used in further reactions or stored in the cytoplasm as free ions. Increasing the concentration of  $P_i$  in the cytoplasm initiates  $P_i$  release through the cell membrane to maintain a tolerable osmotic pressure inside the cells (Rosen and Silver, 1987). Elevated temperature can increase membrane permeability, which in turn facilitates movement of  $P_i$  ions (Bischof et al., 1995). Accordingly, the induced cells' ability to release higher levels of  $P_i$  may relate to the presence of overexpressed PstS protein on the cell surface. As extra  $P_i$  ions can be attached to PstS proteins on the surface, higher levels of  $P_i$  are released once the binding affinity is disrupted (e.g., structural disruption in PstS protein) by an external factor. Therefore, increasing the temperature will facilitate  $P_i$  release and recovery.

361362

363

# 2.3.2 Effect of pH

- Adjusting pH significantly affected  $P_i$  release amongst the cell types, as shown in **Fig. 4b** (two-way ANOVA, p = 0.0092). At pH 5.5 and 7, there was no significant difference in the amount of
- $P_i$  released amongst the cell types (p = 0.087). This pH range has no impact on the intracellular pH
- of E. coli cells, so metabolism, ion transport, and other cellular functions will perform regularly
- 368 (Slonczewski et al., 2009). Furthermore, no difference was expected between the cell types as
- 369 proteins are structurally stable in the circumneutral pH range. In contrast, acidic and basic
- 370 conditions noticeably impacted P<sub>i</sub> release.

- 372 At pH 3.5, the control and uninduced cells released approximately 50% more P<sub>i</sub> than the induced
- cells. In order to lessen the deleterious effects of high proton levels under low pH conditions,
- 374 several molecular strategies are employed for acid resistance (Lund et al., 2014). The most well-
- 375 known strategies are proton pumping, cell membrane modification, production of ammonia and
- proton-consuming decarboxylation reactions, repairing or damage prevention of proteins, and urea
- breakdown (Kanjee and Houry, 2013; Lund et al., 2014). Proton pumping could be a reason for

the increases in P<sub>i</sub> release at low pH observed here. Through this mechanism, protons are exported from the cytoplasm to the extracellular space, which requires energy provided by ATP hydrolysis (Lund et al., 2014). Potential pathways for release of free P<sub>i</sub> ions produced during this reaction might be (i) phosphorylation reactions inside the cell or (ii) active transport outside the cell to neutralize external surface charges. The strong acidic condition affects the surface charge of proteins, providing a positive net surface charge. Consequently, the protein's structure is destabilized, and the protein's functionality is lost (Appling et al., 2016). Although the PstS protein's phosphate-binding site might be disrupted, it is possible that free P<sub>i</sub> ions would be electrostatically attracted to the PstS protein's surface. Hence, less P<sub>i</sub> would be released by the induced cells.

Under basic pH conditions, induced cells offered the highest  $P_i$  release (p = 0.0092). For all cell types, increasing the pH from 8.5 to 10.5 increased  $P_i$  release by approximately 60-70%. Similar to acidic conditions, *E. coli* cells may be capable of several possible passive and active responses to high pH conditions. Three possible categories of actions include chemical processes, metabolic responses, and cell wall destabilization (Claessens et al., 2004). In metabolic responses, proton pumping can be used to prevent proton leakage by actively transporting protons against the concentration gradient. This utilizes ATP as an energy source to initiate proton transport. ATP hydrolysis reactions provide additional free  $P_i$  ions in the cytoplasm. Proton pumping might be responsible for the increased release of  $P_i$  ions. Strong basic conditions affect proteins' surface charge, providing a negative net surface charge. Therefore, the protein's structure will be destabilized, and the protein's functionality will be lost (Appling et al., 2016). The phosphate-binding site of the PstS protein would thus be disrupted, and the bound  $P_i$  ions would be released.

Overall, acidic and basic pH conditions promoted P<sub>i</sub> release, with the PstS protein releasing more P<sub>i</sub> at basic pH levels compared to acidic conditions. These results show that basic conditions may be used for P<sub>i</sub> release and recovery using the cell surface-displayed system.

#### 2.3.3 Effect of Ionic Strength

The impact of ionic strength on  $P_i$  release from all cells is shown in **Fig. 4c**. Desorption of  $P_i$  from all cells significantly increased as ionic strength increased (two-way ANOVA, p = 0.0055).

Induced cells released more P<sub>i</sub> than control and uninduced cells at each ionic strength. The induced cells' P<sub>i</sub> release capacity was approximately 30% to 70% greater than the other cells.

Normally, *E. coli* responds to ionic stress by ion transport and osmotic adjustment (Shabala et al., 2009). Ions can be exchanged (influx/efflux) between the extracellular space and the cytoplasmic pool of ions; cells can also synthesize anions and osmolytes to restore turgor pressure and the normal ionic strength inside the cells (Shabala et al., 2009). Two intracellular possibilities could explain the effect of ionic strength on P<sub>i</sub> desorption. First, simple diffusion of P<sub>i</sub> ions might occur considering that the intracellular concentration of PO<sub>4</sub><sup>3-</sup> is higher than the extracellular concentration. Second, ion exchange with Cl<sup>-</sup> would happen (i.e., Cl<sup>-</sup> influx and PO<sub>4</sub><sup>3-</sup> efflux). These explanations would affect induced, uninduced, and control cells.

The binding affinity of PstS is also affected by ionic strength (Wang et al., 1994). The dissociation constant of the PstS-P<sub>i</sub> complex (K<sub>d</sub>) increases approximately 20-fold at 0.3 mol/L NaCl compared to no-salt solution (Ledvina et al., 1998). Affinity of PstS for anions was found to be insensitive to the surface charge potential of the cleft region (functional site), but extremely sensitive to electrostatic effects at the level of local hydrogen bonding interactions (Ledvina et al., 1998). Thus, increased ionic strength disrupts hydrogen bonds, leading to P<sub>i</sub> release from the binding site. Therefore, induced cells would offer greater P<sub>i</sub> desorption compared to other cells, as observed here.

# 2.4 Phosphorus Adsorption Batch Experiments

Adsorption batch tests were conducted using control cells and induced cells (the uninduced cells were not tested as they performed similarly to the control cells in desorption experiments). The cells' capacity to remove P<sub>i</sub> from solution was investigated following an initial desorption step (starvation, pH & temperature, or enzyme). The pH (10.5) and temperature (40°C) conditions were selected based on the previous desorption batch results. Starvation and enzyme conditions were proposed as additional approaches to be tested. Following desorption, the cells were suspended in two different phosphate solutions (7 mg-PO<sub>4</sub><sup>3</sup>-/L or 70 mg-PO<sub>4</sub><sup>3</sup>-/L; the cells' exhibited low ability to remove P<sub>i</sub> at low initial concentrations, i.e., 1 mg/L), and the resulting P<sub>i</sub> removals are shown in Fig. 5a and Fig. 5b, respectively. Starvation, pH & temperature, and enzymatic conditions were

used to target minimal initial cellular  $P_i$  levels to prepare the *E. coli* cells for  $P_i$  adsorption. The most effective condition to prepare cells for  $P_i$  removal was "starvation," wherein control and induced cells were suspended in 10 mmol/L Tris-HCl solution at pH 7 for approximately 15 hr. This condition effectively released  $P_i$  for induced cells at both  $P_i$  concentrations, but was not effective at 7 mg  $PO_4^{3-}/L$  for control cells (p = 0.636). Under these conditions, additional  $P_i$  ions were released from the control cells (rather than  $P_i$  removal). The free  $P_i$  in the cytoplasm was likely still too high, preventing the cells from uptaking additional  $P_i$ . The induced cells provided approximately 48% additional  $P_i$  removal under starvation conditions with an initial concentration of 70 mg  $PO_4^{3-}/L$ . Starvation conditions may force the cells to consume the pool of free  $P_i$  in the cytoplasm, of which potentially less is available in induced cells compared to control cells. Induced cells would encounter additional stresses during the induction and translocation of fusion protein (INP + PstS), which would require more production of ATP by utilizing the free  $P_i$  in the cytoplasm.

Enzymatic and pH & temperature conditions did not significantly affect adsorption at low  $P_i$  concentrations for either cell type (p = 0.872 and p = 0.991, respectively). However, pH & temperature adjustment was more effective for  $P_i$  adsorption than enzymatic treatment at higher  $P_i$  concentrations. Enzyme addition might only affect the external surrounding and the fusion protein. The PNP enzyme helps to remove free  $P_i$  from solution by converting it to ribose 1-phosphate (Brune et al., 1994). However, pH & temperature adjustment might affect both the internal function of E. coli cells and the fusion protein. Induced cells adsorbed approximately 22% more  $P_i$  than control cells under adjusted pH & temperature conditions. These general observations are in accordance with the expectation that induced cells would adsorb more  $P_i$  than control cells due to the presence of the PstS protein.

# 3. Conclusions

A cell surface-expressed PstS protein system was successfully developed and characterized for  $P_i$  removal and recovery. Increasing temperature (up to 40°C) and ionic strength (up to 1 mol/L) increased phosphate release by 20% and 50%, respectively. Acidic and basic pH conditions also promoted phosphate release, with the PstS protein releasing  $\approx$  63% more phosphate at basic pH levels compared to acidic conditions. Increasing phosphate removal from solution was achieved

when *E. coli* cells were exposed to starvation conditions with low levels of P<sub>i</sub> available. Induced cells provided 48% higher phosphate removal compared to control cells, although removals were generally low.

474

475

476

477

478

479

480

481

471

472

473

Adsorption/desorption results provided proof-of-concept of the feasibility of P<sub>i</sub> release and recovery using cell-surface expressed PstS. However, further studies are needed to optimize performance in order to achieve higher phosphate removal as cellular functions impeded controlled P<sub>i</sub> recovery. Also, investigating other microorganisms targeting more stable induction of the fusion protein is recommended. Inducing mutants in the Pst transport system to confine the cellular interaction might increase the efficiency of the fusion protein in phosphate adsorption and desorption applications. The system must also be tested and optimized for future wastewater/natural water applications.

482 483

484

# **Declaration of Interest**

The authors declare that they have no known competing financial interests or personal relationships that could have appeared to influence the work reported in this paper.

487

488

# **Acknowledgments**

- 489 This work was supported by CAREER award 1554511 from the National Science Foundation
- 490 (NSF). All opinions expressed in this paper are the authors' and do not reflect the views of NSF.
- 491 The authors thank Dr. Martin St. Maurice and Dr. Jodie Box from the Biological Sciences
- Department at Marquette University for their recommendations and help in running Western Blot
- analysis. We also thank Dr. Marcia Silva from Global Water Center at University of Wisconsin-
- 494 Milwaukee and Dr. Marjan Nezafati from the Advanced Analysis Facility at University of
- Wisconsin-Milwaukee for facilitating the use of the FTIR and XPS instruments.

496

497

# Appendix A. Supplementary data

Supplementary data associated with this article can be found in the online version of the paper.

499

# 501 **References**

- 502 APHA, 2005. Standard methods for the examination of water and wastewater, 21st ed. American
- Public Health Association, Washington, D.C.
- 504 Appling, D.R., Anthony-Cahill, S.J., Mathews, C.K., 2016. Biochemistry: Concepts and
- Connections, Global Edi. ed. Pearson Education Limited, Essex, England.
- 506 Bischof, J., Padanilam, J., Holmes, W., Ezzell, R., Lee, R., Tompkins, R., et al., 1995. Dynamics
- of Cell membrane Permeability Changes at Supraphysiological Temperatures. Biophys. J. 68,
- 508 2608–2614.
- Brune, M., Hunter, J.L., Corrie, J.E.T., Webb, M.R., 1994. Direct, Real-Time Measurement of
- Rapid Inorganic Phosphate Release Using a Novel Fluorescent Probe and Its Application to
- 511 Actomyosin Subfragment 1 ATPase. Biochemistry 33, 8262–8271.
- 512 https://doi.org/10.1021/bi00193a013
- 513 Cai, W.J., Hu, X., Huang, W.J., Murrell, M.C., Lehrter, J.C., Lohrenz, S.E., et al., 2011.
- Acidification of subsurface coastal waters enhanced by eutrophication. Nat. Geosci. 4, 766–
- 515 770. https://doi.org/10.1038/ngeo1297
- 516 Choi, S.S., Lee, H.M., Ha, J.H., Kang, D.G., Kim, C.S., Seo, J.H., et al., 2013. Biological removal
- of phosphate at low concentrations using recombinant escherichia coli expressing phosphate-
- binding protein in periplasmic space. Appl. Biochem. Biotechnol. 171, 1170–1177.
- 519 https://doi.org/10.1007/s12010-013-0187-1
- 520 Claessens, J., Behrends, T., Van Cappellen, P., 2004. What do acid-base titrations of live bacteria
- tell us? A preliminary assessment. Aquat. Sci. 66, 19–26. https://doi.org/10.1007/s00027-
- 522 003-0687-0
- 523 Dittrich, M., Sibler, S., 2005. Cell surface groups of two picocyanobacteria strains studied by zeta
- 524 potential investigations, potentiometric titration, and infrared spectroscopy. J. Colloid
- 525 Interface Sci. 286, 487–495. https://doi.org/10.1016/j.jcis.2005.01.029
- 526 Dodds, W.K., Bouska, W.W., Eitzmann, J.L., Pilger, T.J., Pitts, L., Riley, A.J., et al., 2009. Policy
- Analysis Policy Analysis Eutrophication of U. S. Freshwaters: Damages. Environ. Sci.
- 528 Technol. 43, 12–19. https://doi.org/10.1021/es801217q
- 529 Dufrêne, Y.F., Van der Wal, A., Norde, W., Rouxhet, P.G., 1997. X-ray photoelectron
- spectroscopy analysis of whole cells and isolated cell walls of gram-positive bacteria:
- 531 Comparison with biochemical analysis. J. Bacteriol. 179, 1023–1028.

- 532 https://doi.org/10.1128/jb.179.4.1023-1028.1997
- 533 Filip, Z., Hermann, S., Demnerová, K., 2008. FT-IR spectroscopic characteristics of differently
- cultivated Escherichia coli. Czech J. Food Sci. 26, 458–463.
- Guiné, V., Spadini, L., Sarret, G., Muris, M., Delolme, C., Gaudet, J.P., et al., 2006. Zinc sorption
- to three gram-negative bacteria: Combined titration, modeling, and EXAFS study. Environ.
- 537 Sci. Technol. 40, 1806–1813. https://doi.org/10.1021/es0509811
- Haas, J.R., 2004. Effects of cultivation conditions on acid-base titration properties of Shewanella
- putrefaciens. Chem. Geol. 209, 67–81. https://doi.org/10.1016/j.chemgeo.2004.04.022
- Hong, Y., Brown, D., 2006. Cell surface acid-base properties of E. coli and Bacillus brevis and
- variation as a function of growth phase, nitrogen source and C:N ratio. Colloids Surfaces B
- 542 Biointerfaces 50, 112–119.
- Jiang, W., Saxena, A., Song, B., Ward, B.B., Beveridge, T.J., Myneni, S.C.B., 2004. Elucidation
- of functional groups on gram-positive and gram-negative bacterial surfaces using infrared
- 545 spectroscopy. Langmuir 20, 11433–11442. https://doi.org/10.1021/la049043+
- 546 Jung, H.C., Park, J.H., Park, S.H., Lebeault, J.M., Pan, J.G., 1998. Expression of
- carboxymethylcellulase on the surface of Escherichia coli using Pseudomonas syringae ice
- nucleation protein. Enzyme Microb. Technol. 22, 348–354. https://doi.org/10.1016/S0141-
- 549 0229(97)00224-X
- Kanjee, U., Houry, W.A., 2013. Mechanisms of Acid Resistance in Escherichia coli. Annu. Rev.
- 551 Microbiol. 67, 65–81. https://doi.org/10.1146/annurev-micro-092412-155708
- Kozlowski, L.P., 2016. Proteome-pI: Proteome isoelectric point database. Nucleic Acids Res. 45,
- 553 D1112–D1116. https://doi.org/10.1093/nar/gkw978
- Kuroda, A., Kunimoto, H., Morohoshi, T., Ikeda, T., Kato, J., Takiguchi, N., et al., 2000.
- Evaluation of phosphate removal from water by immobilized phosphate-binding protein PstS.
- J. Biosci. Bioeng. 90, 688–690. https://doi.org/10.1016/S1389-1723(00)90020-3
- Langmuir, D., 1997. Aqueous Environmental Geochemistry. Prentice Hall, Upper Saddle River,
- 558 N.J.
- Ledvina, P.S., Tsai, A.L., Wang, Z., Koehl, E., Quiocho, F.A., 1998. Dominant role of local dipolar
- interactions in phosphate binding to a receptor cleft with an electronegative charge surface:
- 561 Equilibrium, kinetic, and crystallographic studies. Protein Sci. 7, 2550–2559.
- 562 https://doi.org/10.1002/pro.5560071208

- Li, L., Kang, D.G., Cha, H.J., 2003. Functional Display of Foreign Protein on Surface of
- Escherichia coli Using N-Terminal Domain of Ice Nucleation Protein. Biotechnol. Bioeng.
- 565 85, 214–221. https://doi.org/10.1002/bit.10892
- Li, Q., Yu, Z., Shao, X., He, J., Li, L., 2009. Improved phosphate biosorption by bacterial surface
- display of phosphate-binding protein utilizing ice nucleation protein. FEMS Microbiol. Lett.
- 568 299, 44–52. https://doi.org/10.1111/j.1574-6968.2009.01724.x
- Lucke, H., Quiocho, F., 1990. High specificity of a phosphate transport protein determined by
- 570 hydrogen bonds. Lett. To Nat. 347, 402–406. https://doi.org/10.1038/346183a0
- 571 Lund, P., Tramonti, A., De Biase, D., 2014. Coping with low pH: Molecular strategies in
- 572 neutralophilic bacteria. FEMS Microbiol. Rev. 38, 1091–1125. https://doi.org/10.1111/1574-
- 573 6976.12076
- Mayer, B.K., Gerrity, D., Rittmann, B.E., Reisinger, D., Brandt-Williams, S., 2013. Innovative
- strategies to achieve low total phosphorus concentrations in high water flows. Crit. Rev.
- 576 Environ. Sci. Technol. https://doi.org/10.1080/10643389.2011.604262
- Ngwenya, B.T., Sutherland, I.W., Kennedy, L., 2003. Comparison of the acid-base behaviour and
- metal adsorption characteristics of a gram-negative bacterium with other strains. Appl.
- 579 Geochemistry 18, 527–538. https://doi.org/10.1016/S0883-2927(02)00118-X
- 580 Ojeda, J.J., Romero-González, M.E., Bachmann, R.T., Edyvean, R.G.J., Banwart, S.A., 2008.
- Characterization of the cell surface and cell wall chemistry of drinking water bacteria by
- combining XPS, FTIR spectroscopy, modeling, and potentiometric titrations. Langmuir 24,
- 583 4032–4040. https://doi.org/10.1021/la702284b
- Omoike, A., Chorover, J., 2004. Spectroscopic study of extracellular polymeric substances from
- Bacillus subtilis: Aqueous chemistry and adsorption effects. Biomacromolecules 5, 1219–
- 586 1230. https://doi.org/10.1021/bm034461z
- Park, M., Yoo, G., Bong, J.H., Jose, J., Kang, M.J., Pyun, J.C., 2015. Isolation and characterization
- of the outer membrane of Escherichia coli with autodisplayed Z-domains. Biochim. Biophys.
- Acta Biomembr. 1848, 842–847. https://doi.org/10.1016/j.bbamem.2014.12.011
- Rittmann, B.E., Mayer, B., Westerhoff, P., Edwards, M., 2011. Capturing the lost phosphorus.
- 591 Chemosphere 84, 846–853. https://doi.org/10.1016/j.chemosphere.2011.02.001
- Rosen, B.P., Silver, S., 1987. Ion Transport in Prokaryotes. Academic Press, Inc., California.
- 593 Shabala, L., Bowman, J., Brown, J., Ross, T., McMeekin, T., Shabala, S., 2009. Ion transport and

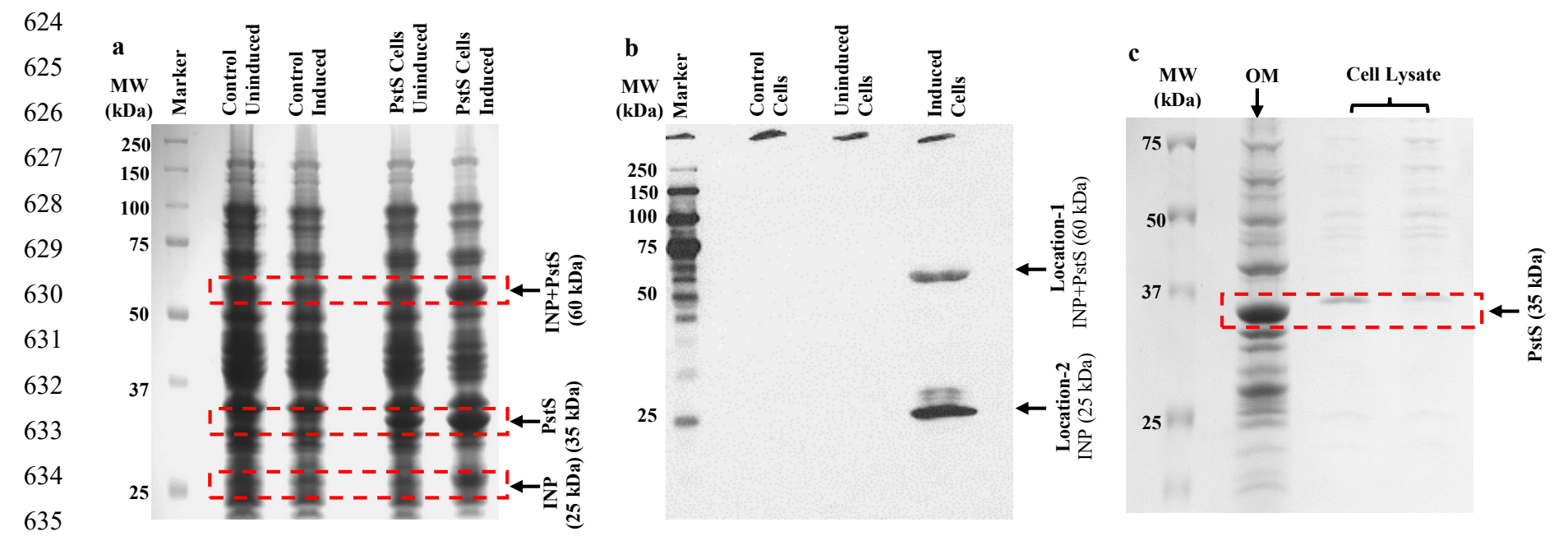
- 594 osmotic adjustment in Escherichia coli in response to ionic and non-ionic osmotica. Environ. 595 Microbiol. 11, 137–148. 596 Slonczewski, J., Fujisawa, M., Dopson, M., Krulwich, T., 2009. Cytoplasmic pH Measurement 597 and Homeostasis in Bacteria and Archaea. Adv. Microb. Physiol. 55, 1-317. 598 https://doi.org/10.1016/S0065-2911(09)05501-5 599 Turner, B.F., Fein, J.B., 2006. Protofit: A program for determining surface protonation constants 600 from titration data. Comput. Geosci. 32, 1344-1356. 601 https://doi.org/10.1016/j.cageo.2005.12.005 602 Van Der Mei, H.C., De Vries, J., Busscher, H.J., 2000. X-ray photoelectron spectroscopy for the 603 study of microbial cell surfaces. Surf. Sci. Rep. 39, 1-24. https://doi.org/10.1016/S0167-604 5729(00)00003-0 605 Venkiteshwaran, K., Pokhrel, N., Hussein, F., Antony, E., Mayer, B.K., 2018. Phosphate removal 606 and recovery using immobilized phosphate binding proteins. Water Res. X 1, 100003. 607 https://doi.org/10.1016/j.wroa.2018.09.003 608 Wang, Z., Choudhary, A., Ledvina, P.S., Quiocho, F.A., 1994. Fine tuning the specificity of the
- periplasmic phosphate transport receptor. Site-directed mutagenesis, ligand binding, and
  crystallographic studies. J. Biol. Chem. 269, 25091–25094.
  Yang, Y., Ballent, W., Mayer, B.K., 2016. High-affinity phosphate-binding protein (PBP) for
- phosphorous recovery: Proof of concept using recombinant Escherichia coli. FEMS Microbiol. Lett. 363, 1–6. https://doi.org/10.1093/femsle/fnw240

# **List of Tables**

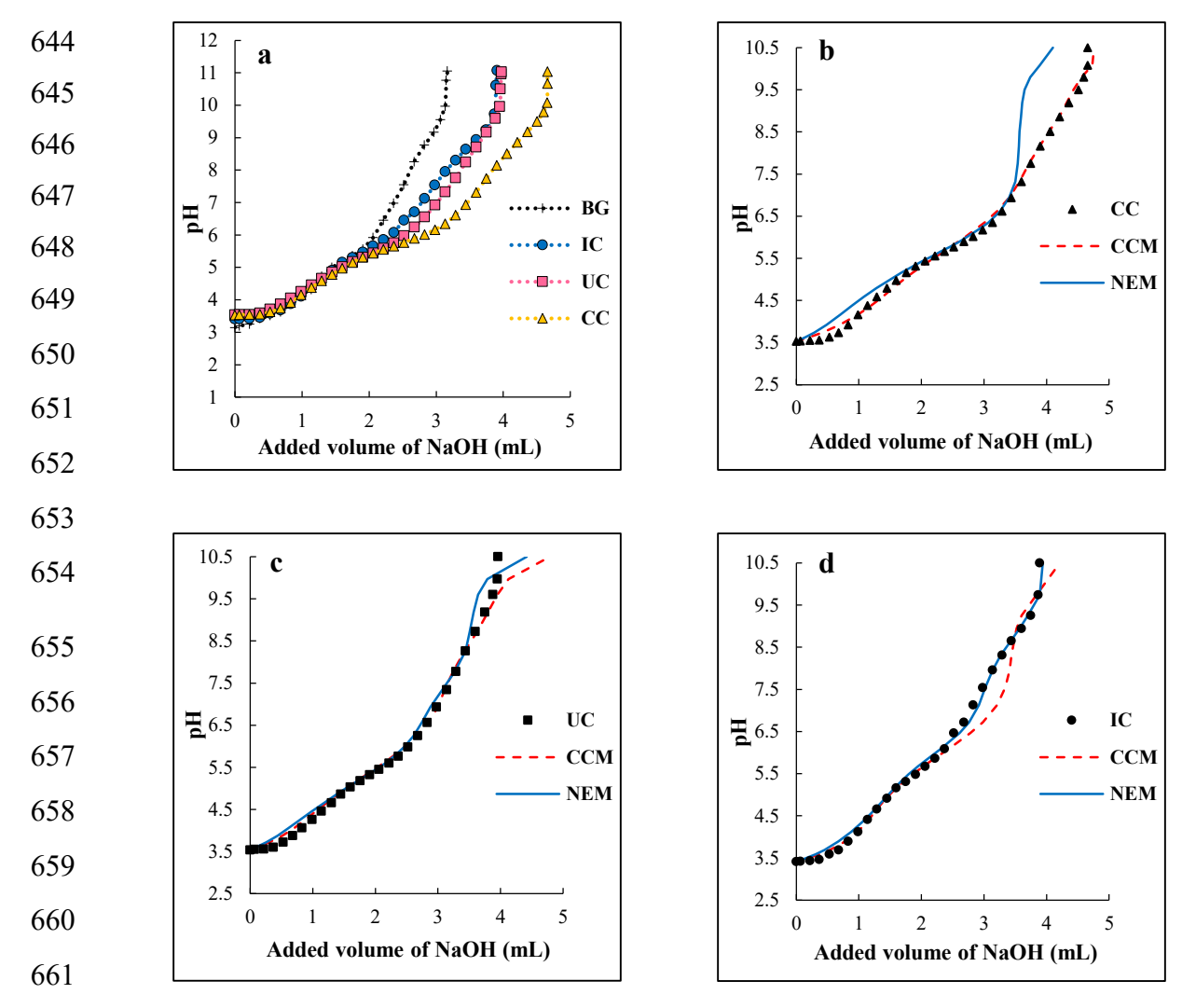
Table 1
 Deprotonation constants (pK<sub>a</sub>) and point of zero charge (pH<sub>pzc</sub>) as calculated with ProtoFit GIU
 using the constant capacitance model (CCM) and non-electrostatic model (NEM) for control cells,
 uninduced cells, and induced cells.

Cell Type	Cons	Constant Capacitance Model (CCM)				Non-Electrostatic Model (NEM)			
	pK <sub>a1</sub>	$pK_{a2}$	pK <sub>a3</sub>	$pH_{pzc}$	•	$pK_{a1}$	pK <sub>a2</sub>	$pK_{a3}$	$pH_{pzc}$
Control Cells	3.88	5.81	8.08	5.91	•	4.50	5.50	6.15	6.11
Uninduced Cells	3.15	5.45	8.05	5.54		4.45	5.36	7.46	6.75
Induced Cells	3.20	5.99	9.75	6.08		4.40	6.00	8.58	7.73

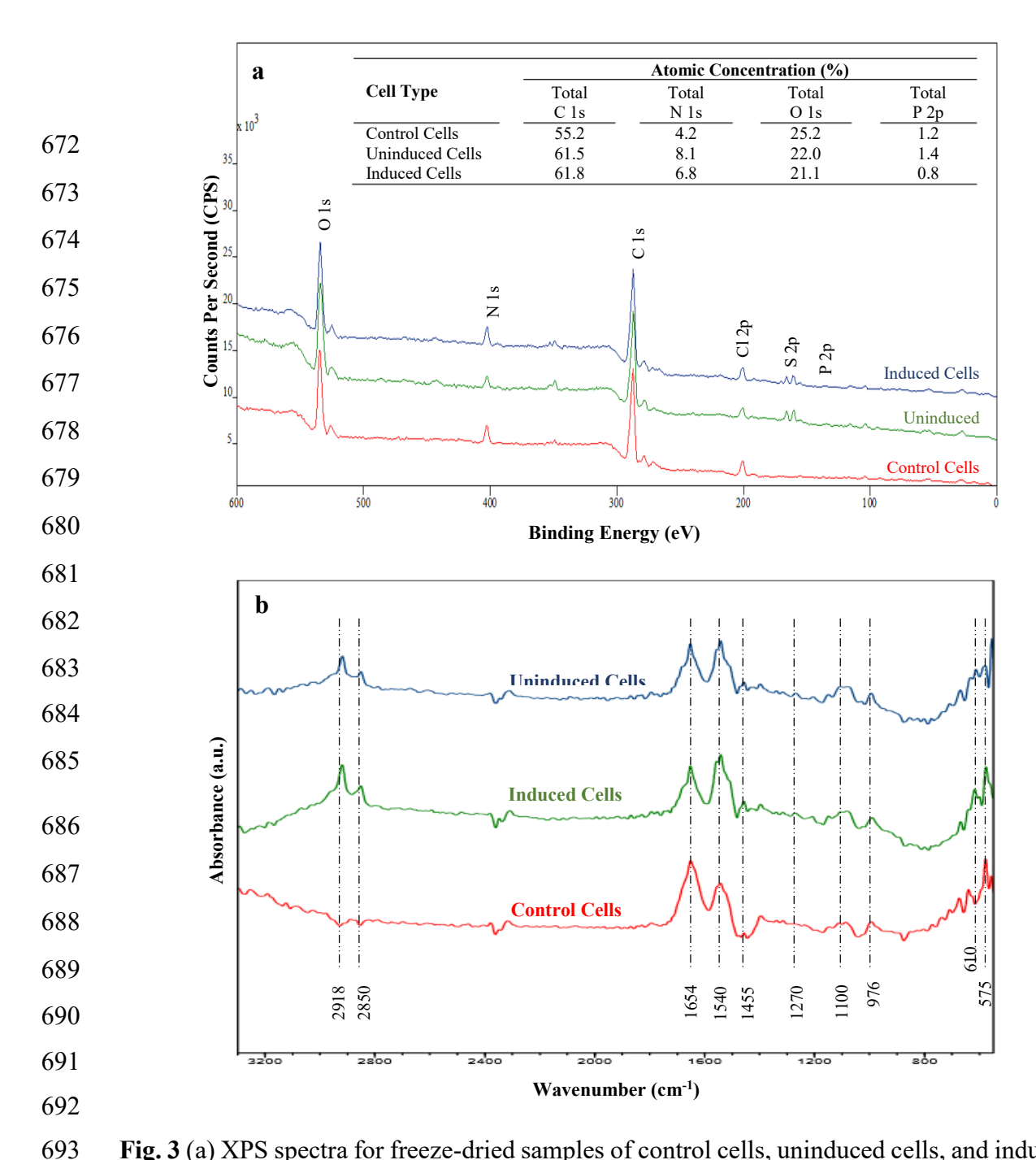
# **List of Figures**



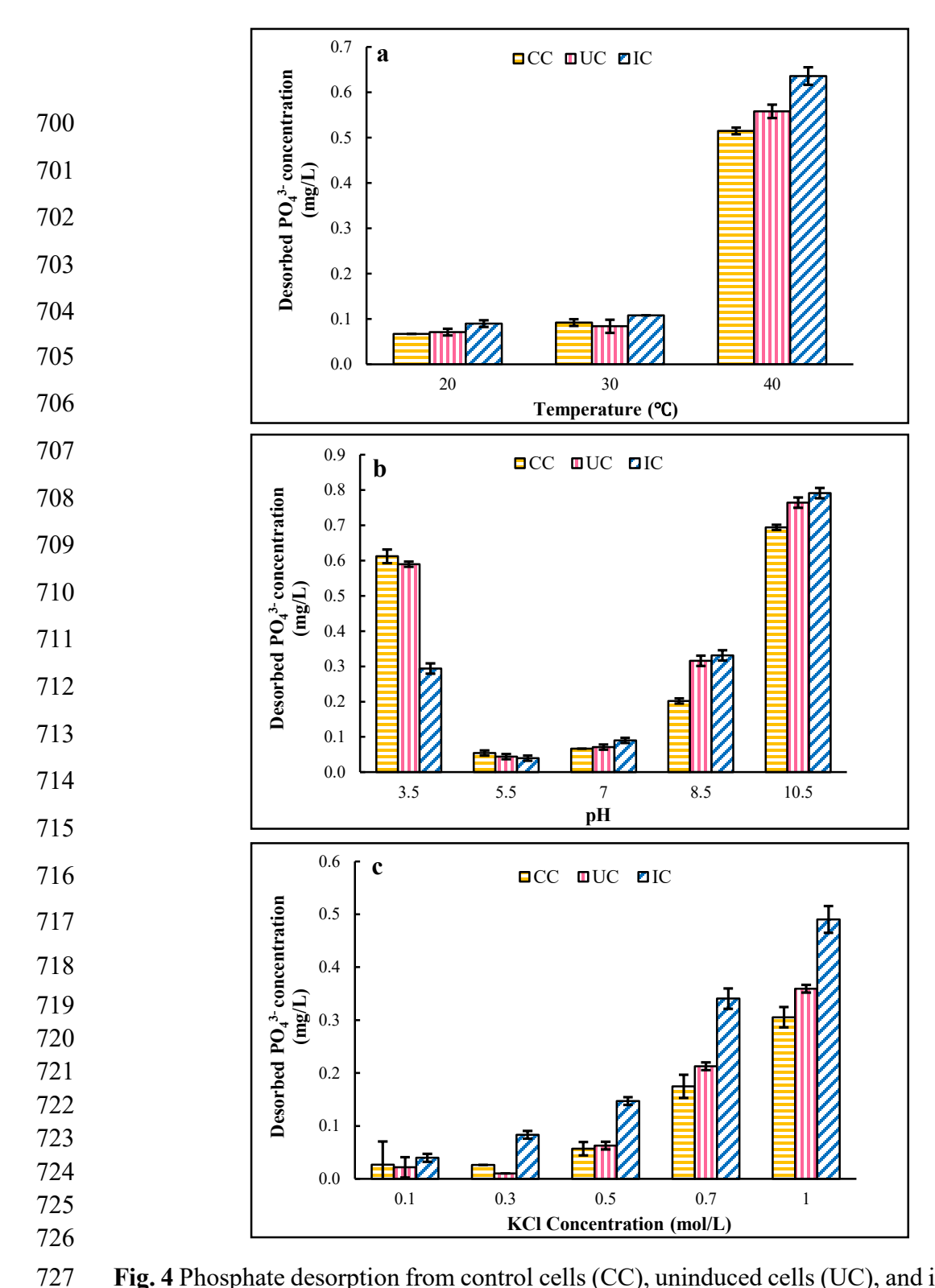
**Fig. 1** Protein verification, expression, and separation analyses. (a) Protein verification using SDS-PAGE analysis of control cells (lane 2: before IPTG induction [Control Uninduced]; lane 3: after IPTG induction [Control Induced]) and PstS cells (lane 4: before IPTG induction [PstS Cells Uninduced]; lane 5: after IPTG induction [PstS Cells Induced]). Lane 1 is the protein marker. (b) Protein expression using Western Blot analysis shows two distinguished bands for the induced cells, corresponding to INP only and INP + PstS together. (c) SDS-PAGE analysis of the outer membrane (OM) separation analysis of the induced cells showing the presence of PstS in the OM fraction rather than the cell lysate fraction.



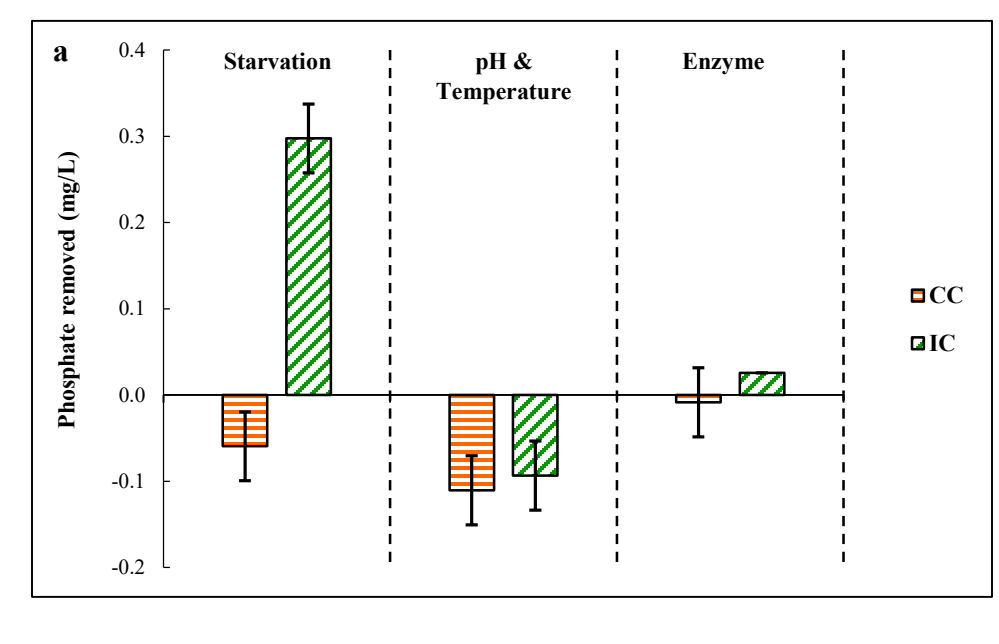
**Fig. 2** (a) Typical acid-base titration curves for induced cells (IC), uninduced cells (UC), and control cells (CC) suspended in 0.01 mol/L NaCl with final  $OD_{600} = 2$ . BG = background solution (0.1 mol/L NaCl). (b), (c), and (d) three-site (2 acid and 1 base) constant capacitance model (CCM) and three-site (2 acid and 1 base) non-electrostatic model (NEM) curve fits for CC, UC, and IC, respectively.



**Fig. 3** (a) XPS spectra for freeze-dried samples of control cells, uninduced cells, and induced cells. Acquisition with pass energy 100 eV and 1 eV step size using Mg K $\alpha$  X-ray source. The inset table shows the percentage atomic concentration of C, N, O, and P on the bacterial surface calculated from the XPS spectra. (b) Infrared spectra of control cells, uninduced cells, and induced cells suspension in 10 mmol/L Tris-HCl solution at a final OD<sub>600</sub> = 2. The spectra are vertically offset for clarity. Peaks were identified and functional groups were assigned as shown in the Supplementary Data Table S2.



**Fig. 4** Phosphate desorption from control cells (CC), uninduced cells (UC), and induced cells (IC) with final  $OD_{600} = 1$  as a function of (a) temperature, (b) pH, and (c) ionic strength. All experiments were conducted in triplicate, and error bars denote  $\pm 1$  standard deviation.



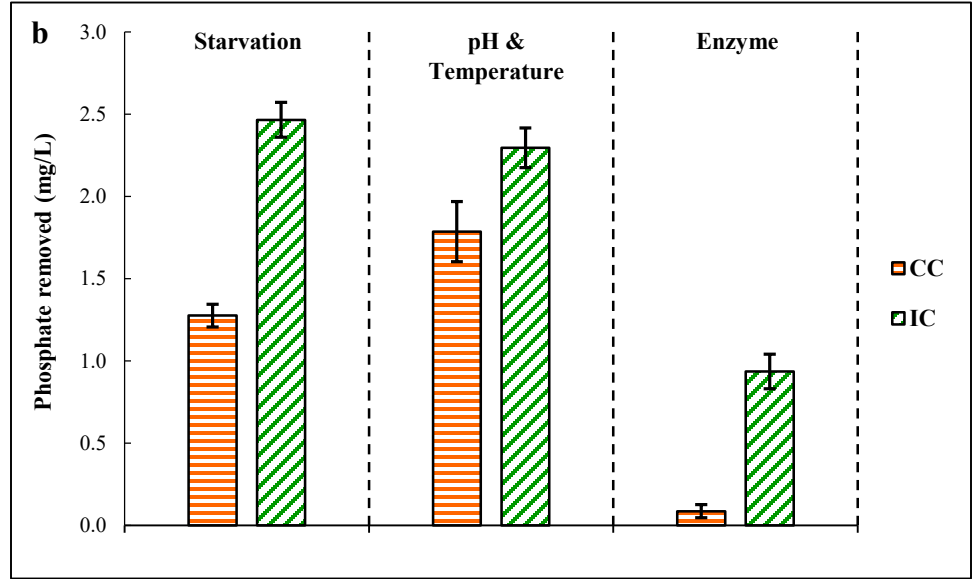


**Fig. 5** Phosphate uptake by control cells and induced cells after desorption conditions (starvation, pH & temperature, and enzyme). Two phosphate concentrations were selected for adsorption tests (a) 7 mg  $PO_4^{3-}/L$  and (b) 70 mg  $PO_4^{3-}/L$ . All phosphate adsorption experiments were conducted in triplicate for 3 hr at room temperature, 250 r/min mixing, and pH 6.7. Error bars denote  $\pm 1$  standard deviation.